

## Increasing the $Q$ factor in the constant-excitation mode of frequency-modulation atomic force microscopy in liquid

D. Ebeling and H. Hölscher<sup>a)</sup>

Center for Nanotechnology (CeNTech), Heisenbergstr. 11, 48149 Münster, Germany and Physikalisches Institut, Westfälische Wilhelms-Universität Münster, Wilhelm-Klemm-Str. 10, 48149 Münster, Germany

B. Anczykowski

nanoAnalytics GmbH, Heisenbergstr. 11, 48149 Münster, Germany

(Received 15 August 2006; accepted 30 September 2006; published online 16 November 2006)

By adding a  $Q$ -control electronics to the setup of the constant-excitation mode of the frequency-modulation atomic force microscope, the authors are able to increase the effective  $Q$  factor of a self-oscillated cantilever in liquid to values comparable to ambient conditions. During imaging of soft biological samples adsorbed on a mica substrate, the authors observed an increased corrugation of the topography with increased  $Q$  factors. This effect is caused by the reduction of tip-sample indentation forces as demonstrated by numerical simulations and an analytical approach. © 2006 American Institute of Physics. [DOI: 10.1063/1.2387122]

In *atomic force microscopy*<sup>1</sup> (AFM) it is a common approach to oscillate the cantilever near the sample surface in order to avoid unwanted lateral forces between tip and sample surface during scanning. For applications in vacuum the *frequency-modulation* (FM) technique<sup>2</sup> became the standard driving technique during the last decade. The FM technique is based on the specific properties of a self-driven oscillator<sup>3-7</sup> and can be divided into the constant-amplitude<sup>2</sup> and constant-excitation<sup>8</sup> modes.

Although the FM technique was originally introduced for applications in vacuum where the natural  $Q$  factors of the cantilever are high, the frequency-modulation technique can be also applied under ambient conditions<sup>9,10</sup> and in liquids<sup>11,12</sup> where the cantilever is damped by the surrounding media. The advantage of this approach compared to the often applied amplitude-modulation or “tapping” mode<sup>13-15</sup> is the possibility to perform continuous and quantitative spectroscopy of tip-sample force curves<sup>10,16</sup> in addition to topography imaging.

Here we show how the effective  $Q$  factor of a self-driven cantilever can be increased in the the constant-excitation mode of the FM technique. While imaging a *L-a*-dipalmitoylphosphatidylcholine (DPPC) bilayer and DNA adsorbed on mica with increased  $Q$  factors, we observed an increase of the measured topography for higher  $Q$  values. This effect can be explained by the reduction of tip-sample indentation and force by the increased  $Q$  factor as shown by simulations and an analytical analysis.

A sketch of the experimental setup of an atomic force microscope utilizing the FM technique with  $Q$  control is shown in Fig. 1. The deflection of the cantilever is measured with the laser beam deflection method and this signal is subsequently used to excite the cantilever by a piezo. For this purpose an external electronics consisting of a time (or phase) shifter and an automatic gain control is used. Since we apply the constant-excitation (CE) mode, the driving amplitude is kept at a constant value  $a_{\text{exc}}$  by the electronics. In order to control the effective  $Q$  factor of the system, we added an additional feedback circuit consisting also of an amplifier and a time shifter. The  $Q$ -control feedback ampli-

fies the oscillation signal of the cantilever by a constant gain factor  $g$ . This signal is added to the conventional driving signal of the constant-excitation mode. However, it is important to clarify that both driving mechanisms amplify the oscillation signal of the cantilever in a different way. The amplification of the  $Q$ -control feedback by a constant gain factor results in an amplitude dependent driving signal, while the amplification of the CE-mode feedback results in a driving signal independent of the actual oscillation amplitude.

Consequently, the two driving mechanisms are reflected by two different terms in the corresponding equation of motion

$$m\ddot{z}(t) + \frac{2\pi f_0 m}{Q_0} \dot{z}(t) + c_z z(t) + \underbrace{g c_z z(t-t_0)}_{Q \text{ control}} + \underbrace{\frac{a_{\text{exc}}}{A} c_z z(t-t_0)}_{\text{CE mode}} = \underbrace{F_{\text{ts}}[z(t)]}_{\text{tip-sample force}}. \quad (1)$$

Here,  $z(t)$  is the position of the tip at time  $t$ ;  $c_z$ ,  $m$ ,  $Q_0$ , and  $f_0 = \sqrt{(c_z/m)}/(2\pi)$  are the spring constant, the effective mass, the quality factor, and the eigenfrequency of the cantilever, respectively. Equation (1) is the equation of motion for the CE modes,<sup>17</sup> where we added the  $Q$ -control driving term.<sup>18</sup> The retarded displacement signal  $z(t-t_0)$  is amplified by a factor  $a_{\text{exc}}/A$  for the description of the constant-excitation mode, while it is multiplied by a constant gain factor  $g$  in the  $Q$ -control term. For simplicity we consider the same time shift  $t_0$  for both. The tip-sample interaction force  $F_{\text{ts}}$  is introduced by the last term.

In order to establish the basic principles of  $Q$  control in the FM technique, we first analyze a cantilever oscillating far away from the sample surface. In this case there are no forces interacting between tip and sample (i.e.,  $F_{\text{ts}}=0$ ), which simplifies the equation of motion [Eq. (1)]. Further simplification arises by considering only stable, steady-state solutions for  $t \gg 0$ , where the cantilever oscillates sinusoidally and with constant amplitude  $A$ . Therefore, we use the ansatz  $z(t)=A \cos(2\pi f t)$  to solve the equation of motion (1). As a result, we obtain a system of two coupled trigonometric equations:

<sup>a)</sup>Electronic mail: hendrik.hoelscher@uni-muenster.de

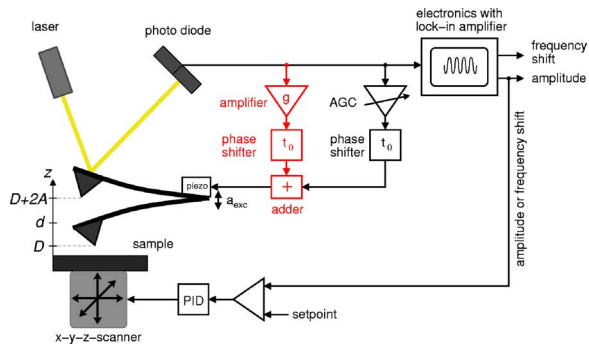


FIG. 1. (Color online) Schematic drawing of the experimental setup showing a dynamic force microscope using the constant-excitation mode with  $Q$  control. The tip oscillates between the nearest tip-sample position  $D$  and  $D+2A$ . The equilibrium position of the tip is denoted as  $d$ . The additional feedback for  $Q$  control is shown in red.

$$(f^2 - f_0^2)/f_0^2 = (g + a_{exc}/A)\cos(2\pi ft_0), \quad (2a)$$

$$f/(f_0 Q_0) = (g + a_{exc}/A)\sin(2\pi ft_0). \quad (2b)$$

These coupled equations greatly simplify if the time shift is set to an optimal value of  $t_0 = 1/(4f_0)$  corresponding to  $90^\circ$ . In this case the cantilever oscillates exactly with its eigenfrequency  $f=f_0$  and the oscillation amplitude is given by

$$A = a_{exc}/(1/Q_0 - g) = a_{exc}Q_{eff}, \quad (3)$$

where we defined the effective  $Q$  factor as  $Q_{eff} = 1/(1/Q_0 - g)$ . This definition is analogous to the effective  $Q$  factor already defined for  $Q$  control in the tapping mode.<sup>10,18,19</sup>

Analyzing the features of  $Q$  control in the FM mode, we found that the increase of the effective  $Q$  factor has a profound influence on the tip-sample interaction. Our study is based on the imaging of several samples with increased  $Q$  factors in ambient conditions as well as in liquids. The overall effect, however, is most prominent for soft biological samples adsorbed on a harder substrate. In contrast to the FM mode in vacuum where the frequency shift is typically used as a feedback signal to scan the sample surface, we use the oscillation amplitude as a feedback signal under ambient conditions and in liquids.<sup>10</sup> Analyzing the resulting topography images in liquid we observed a very systematic increase of the measured height of soft samples on harder substrates.

Figure 2 shows a comparison between the CE mode without and with additional  $Q$  control obtained on DNA and a DPPC bilayer adsorbed on mica in liquids. The experiments were performed with a commercial atomic force microscope (NanoScope IIIa with MultiMode head, Veeco Instruments Inc.) equipped with a liquid cell. Self-developed electronics were used to drive the cantilever in constant-excitation mode without and with  $Q$  control. The samples were scanned with rectangular silicon cantilevers ( $c_z = 3 \text{ N/m}$ ,  $f_0 = 75 \text{ kHz}$ ). During imaging we choose the highest possible values for the set points for the standard CE mode and with additional  $Q$  control. In this context, “highest possible” refers to the fact that with higher set points the tip was not tracking the surface correctly and no clear contrast could be achieved for imaging. By the application of this procedure we tried to keep the tip-sample interaction as low

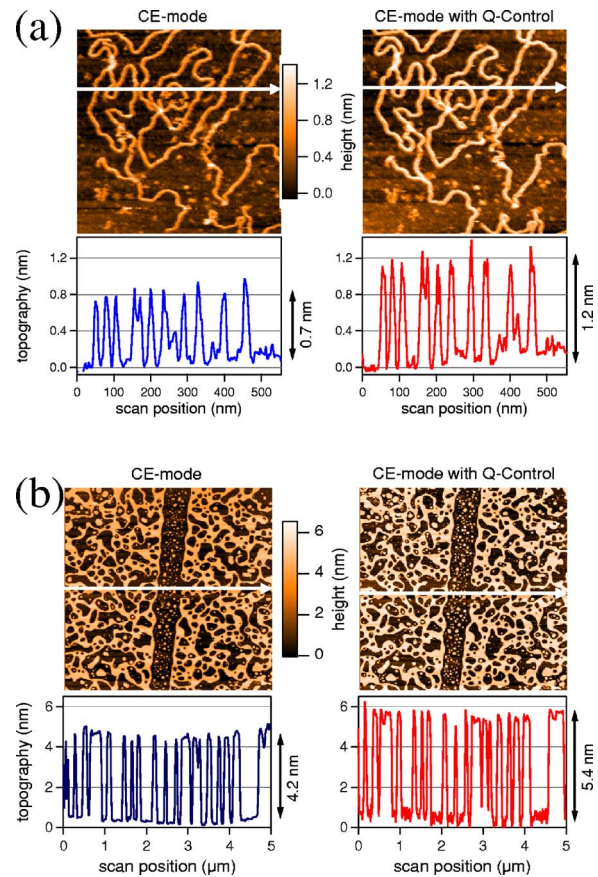


FIG. 2. (Color online) Comparison between CE mode without (left) and with  $Q$  control (right). (a) Increasing the effective  $Q$  factor from 64 to 241, the measured height of the DNA in EB buffer increased from 0.7 to 1.2 nm. (b) The measured height of the bilayer of DPPC increased from  $4.2 \pm 0.2 \text{ nm}$  in the conventional CE mode ( $Q_0 = 58$ ) to  $5.4 \pm 0.2 \text{ nm}$  with  $Q$  control ( $Q_{eff} = 240$ ).

as possible. All images were measured with a scan velocity of 1 Hz and with individually optimized gains (see Ref. 20).

Analyzing the height of the adsorbed DNA we found a significant increase from 0.7 to 1.2 nm without and with  $Q$  control, respectively. The free oscillation amplitude in the CE mode was about 0.63 V ( $\approx 7 \text{ nm}$ ). In order to keep the free oscillation amplitude with  $Q$  control to a comparable value of 0.59 V, we had to reduce the excitation amplitude  $a_{exc}$  of the CE mode. By adding the  $Q$  control driving we increased the  $Q$  factor from 64 to 241. Images presented in Fig. 2 were measured with a set point of 0.57 V (CE mode) and 0.4 V ( $Q$  control).

The same effect is also observed for a DPPC bilayer in water adsorbed on a mica substrate. In this case the measured height increases from 4.2 to 5.2 nm, while the  $Q$  factor was increased from 58 to 240. The free oscillation amplitude in the CE mode was set to 1.5 V ( $\approx 18 \text{ nm}$ ). During imaging we choose the highest possible values for the set points for the CE mode (1.1 V) and with additional  $Q$  control (0.95 V).

This increase of the measured height of the DNA and the DPPC can be readily explained by the reduction of the tip-sample interaction. The dependency of the tip-sample forces on the measured height has been previously examined for DNA (Ref. 21) and DPPC (Ref. 22) for conventional tapping mode. In frequency-modulation AFM the tip-sample indentation depends strongly on the actual  $Q$  factor as demonstrated by numerical simulations based on the equation of motion [Eq. (1)]. For these calculations we modeled the tip-

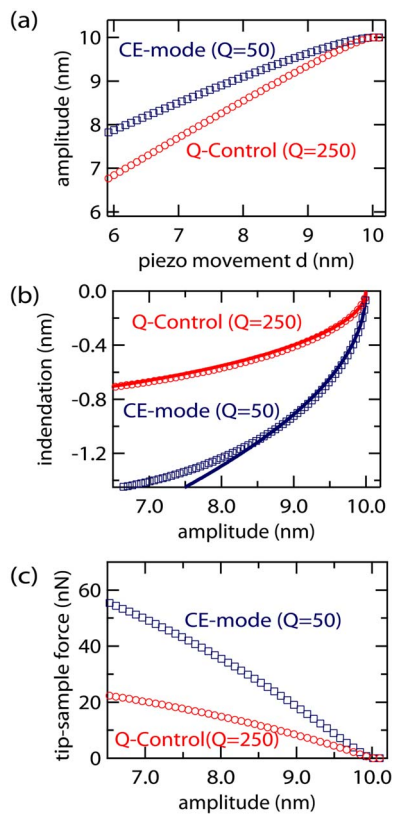


FIG. 3. (Color online) Comparison of (a) the oscillation amplitude, (b) the tip-sample indentation, and (c) the tip-sample force at the turning point  $D$  obtained in the conventional CE mode ( $Q_0=50$ ) and with additional  $Q$  control ( $Q_{\text{eff}}=250$ ) in a liquid environment. The curves change significantly with dependence on the  $Q$  factor. The analytical relationship [Eq. (4)] between the tip-sample indentation and oscillation amplitude is plotted as a solid line in (b).

sample interaction in liquids by the well known Hertz model,  $F_{\text{Hertz}}(z) = \frac{4}{3}E^*\sqrt{R}(-z)^{3/2}$  for  $z < 0$ , where  $R$  is the tip radius and  $E^*$  the effective modulus.<sup>23</sup> Figure 3 displays the resulting spectroscopy curves, where we choose parameters close to the experiments:  $c_z = 3.0 \text{ N/m}$ ,  $f_0 = 75.0 \text{ kHz}$ ,  $Q_0 = 50$ ,  $g = 0.8/Q_0 \Rightarrow Q_{\text{eff}} = 250$ ,  $R = 10 \text{ nm}$ ,  $E_s = 10 \text{ GPa}$ ,  $E_t = 130 \text{ GPa}$ , and  $\mu_{t,s} = 0.3$ .

A comparison between the results without and with  $Q$  control reveals a significant difference between the amplitude and distance curves [Fig. 3(a)]. As the cantilever sample position  $d$  is decreased, the oscillation amplitude  $A$  decreases considerably faster for an increased  $Q$  factor. This effect has a direct consequence for the resulting tip-sample indentation [Fig. 3(b)]. Assuming for example, an amplitude of 7 nm as set point, the indentation reaches  $-1.4 \text{ nm}$  for a natural  $Q$  factor of 50, while it is below  $-0.7 \text{ nm}$  for an increased effective  $Q$  factor of 250. Consequently, the tip-sample forces are also greatly reduced with increased  $Q$  factors. Figure 3(c) shows the maximal tip-sample force at the turning point  $D$  as a function of the actual oscillation amplitude  $A$ . The forces with  $Q$  control are significantly lower compared to the values without additional feedback.

The decrease of the tip-sample indentation with increasing effective  $Q$  factor can be additionally demonstrated by an analytical analysis of the equation of motion. Developing the tip-sample force into a Fourier series and assuming the so-called large-amplitude limit for the Hertzian force law,<sup>24</sup> the tip-sample indentation can be calculated as

$$D(A) = -\sqrt{\sqrt{\frac{2c_z A^{3/2}}{R E^*} \left( \left( 1 - \frac{Q_0}{Q_{\text{eff}}} + \frac{Q_0 A_0}{Q_{\text{eff}} A} \right)^2 - 1 \right)}}. \quad (4)$$

This equation reveals the relationship between tip-sample indentation and effective  $Q$  factor. In addition, the indentation depends on various other parameters such as elastic modulus, tip radii, spring constant, and oscillation amplitude. The agreement between the simulations and this analytical formula is shown in Fig. 3(b).

In summary, we presented a technique to modify the effective  $Q$  factor in the constant-excitation mode of the frequency-modulation technique. This approach enables the increase of the  $Q$  factor in liquids to values comparable to ambient conditions. Measuring the height of DNA and DPPC adsorbed on a mica substrate, we observed a significant increase of the topography with increased effective  $Q$  factors. As shown by numerical simulations and an analytical approach, this feature of  $Q$  control can be explained by the reduction of the tip-sample indentation and force.

The authors acknowledge continuous support and many helpful discussions with André Schirmeisen, Jan-Erik Schmutz, Marcus Schäfer, and Harald Fuchs. This project was financially supported by the German Federal Ministry of Education and Research (BMBF) (Grant No. 03N8704).

- <sup>1</sup>G. Binnig, C. F. Quate, and C. Gerber, *Phys. Rev. Lett.* **56**, 930 (1986).
- <sup>2</sup>T. R. Albrecht, P. Grütter, D. Horne, and D. Rugar, *J. Appl. Phys.* **69**, 668 (1991).
- <sup>3</sup>A. Metha, S. Cherian, D. Hedden, and T. Thundat, *Appl. Phys. Lett.* **78**, 1637 (2001).
- <sup>4</sup>H. Hölscher, B. Gotsmann, W. Allers, U. D. Schwarz, H. Fuchs, and R. Wiesendanger, *Phys. Rev. B* **64**, 075402 (2001).
- <sup>5</sup>G. Muralidharan, A. Metha, S. Cherian, and T. Thundat, *J. Appl. Phys.* **89**, 4587 (2001).
- <sup>6</sup>H. Hölscher, B. Gotsmann, W. Allers, U. D. Schwarz, H. Fuchs, and R. Wiesendanger, *Phys. Rev. Lett.* **88**, 019601 (2002).
- <sup>7</sup>A. Passian, G. Muralidharan, S. Kouchejian, A. Metha, S. Cherian, T. L. Ferrel, and T. Thundat, *J. Appl. Phys.* **91**, 4693 (2002).
- <sup>8</sup>H. Ueyama, Y. Sugawara, and S. Morita, *Appl. Phys. A: Mater. Sci. Process.* **66**, S295 (1998).
- <sup>9</sup>K. Kobayashi, H. Yamada, and K. Matsushige, *Appl. Surf. Sci.* **188**, 430 (2002).
- <sup>10</sup>H. Hölscher and B. Anczykowski, *Surf. Sci.* **579**, 21 (2005).
- <sup>11</sup>H. Sekiguchia, T. Okajimaa, H. Arakawaa, S. Maedab, A. Takashimab, and A. Ikai, *Appl. Surf. Sci.* **210**, 61 (2003).
- <sup>12</sup>T. Okajima, H. Sekiguchi, H. Arakawa, and A. Ikai, *Appl. Surf. Sci.* **210**, 68 (2003).
- <sup>13</sup>Y. Martin, C. C. Williams, and H. K. Wickramasinghe, *J. Appl. Phys.* **61**, 4723 (1987).
- <sup>14</sup>Q. D. Zhong, D. Inniss, K. Kjoller, and V. B. Elings, *Surf. Sci. Lett.* **290**, L688 (1993).
- <sup>15</sup>C. A. J. Putman, K. O. Vanderwerf, B. G. Degrooth, N. F. Vanhulst, and J. Greve, *Appl. Phys. Lett.* **64**, 2454 (1994).
- <sup>16</sup>T. Uchihashi, M. J. Higgins, S. Yasuda, S. P. Jarvis, S. Akita, Y. Nakayama, and J. E. Sader, *Appl. Phys. Lett.* **85**, 3575 (2004).
- <sup>17</sup>H. Hölscher, B. Gotsmann, and A. Schirmeisen, *Phys. Rev. B* **68**, 153401 (2003).
- <sup>18</sup>H. Hölscher, D. Ebeling, and U. D. Schwarz, *J. Appl. Phys.* **99**, 084311 (2006).
- <sup>19</sup>T. R. Rodríguez and R. García, *Appl. Phys. Lett.* **82**, 4821 (2003).
- <sup>20</sup>D. Ebeling, H. Hölscher, H. Fuchs, B. Anczykowski, and U. D. Schwarz, *Nanotechnology* **17**, S221 (2006).
- <sup>21</sup>B. Pignataro, L. F. Chi, S. Gao, B. Anczykowski, C. Niemeyer, M. Adler, and H. Fuchs, *Appl. Phys. A: Mater. Sci. Process.* **74**, 447 (2002).
- <sup>22</sup>M. Hartig, L. F. Chi, X. D. Liu, and H. Fuchs, *Thin Solid Films* **327–329**, 262 (1998).
- <sup>23</sup>The effective modulus is defined as  $E^* = ((1 - \mu_t^2)/E_t + (1 - \mu_s^2)/E_s)^{-1}$  depending on the elastic moduli  $E_{t,s}$  and the Poisson ratios  $\mu_{t,s}$  of tip and sample, respectively.
- <sup>24</sup>H. Bielefeldt and F. J. Giessibl, *Surf. Sci. Lett.* **440**, L863 (1999).